

# Conductance of a Conjugated Molecule with Carbon Nanotube Contacts

Nicolas A. Bruque,\* M. K. Ashraf, and Roger K. Lake

*Department of Electrical Engineering,  
University of California Riverside, CA 92521*

## Abstract

Calculations of the conductance of a carbon nanotube (CNT)-molecule-CNT structure are in agreement with experimental measurements [1]. The features in the transmission correspond directly to the features of the isolated molecular orbitals. The HOMO provides conductance at low bias that is relatively insensitive to the end groups of the cut CNTs, the cut angle, or the number of molecular bridges. A molecular conformation change not directly in the path of the carrier transport increases the resistance by over 2 orders of magnitude.

*Keywords:* Electron transport, FIREBALL, CNT, DFT, NEGF, conductance, molecular electronics

---

\*Electronic address: nbruque@ee.ucr.edu

Individual molecules have been proposed as the ultimately scaled electronic device in future electronics. Gold metal contacts to molecules has been studied the longest and given the most attention both experimentally and theoretically [2, 3, 4, 5]. The agreement between the experimentally measured currents and the theoretically predicted currents in these systems was difficult to obtain due to the strong dependence of the conductance on the contact geometry [5, 6, 7, 8, 9, 10]. The correspondence has greatly improved with the introduction of amine linkers [11, 12, 13].

The carbon nanotube (CNT) has been utilized as an alternative contact to single molecules [1, 14, 15]. The CNT-molecule-CNT amide interface chemistry provides a well defined covalent bond to attach CNT contacts to single molecules. The CNT contacts can provide both metallic and semiconducting properties governed by the CNT chirality.

Prior transport studies report that the current response of CNT-molecule-CNT systems is greatly influenced by the chirality of the CNT contacts [16, 17, 18] while others report changes when examining the passivation chemistry at the cut ends of the CNTs [19]. The CNT-molecule-CNT transport studies published to date have been limited to model or proposed systems [16, 17, 18, 19, 20, 21, 22, 23] where the CNT-molecule interface chemistry, interface geometry, CNT chirality, or molecular conformation were the areas of focus. Comparisons between theory and experiment for these systems have not yet been performed. In this paper we present transport calculations of a CNT-molecule-CNT system that was built and measured [1], we make quantitative comparisons, and we show how the features in the transmission spectrum result from the features of the molecular orbitals of the isolated molecules.

To calculate the equilibrium transmission of a CNT-molecule-CNT system, our method uses density functional theory (DFT) implemented by the *ab initio* tight-binding molecular dynamics code FIREBALL [24, 25, 26] coupled with a non-equilibrium Green's functional (NEGF) algorithm [21, 27, 28, 29, 30]. The BLYP exchange-correlation functional is used to perform a self-consistent calculation [31, 32] using a double numeric  $sp^3$  localized orbital FIREBALL basis. We relax the system using periodic boundary conditions until forces are  $< 0.05 \text{ eV } \text{Å}^{-1}$  using a self-consistent convergence factor of  $10^{-5}$ . These matrix elements are used to calculate the surface self-energies, Green's function of the device, and the resulting transmission. To calculate the room temperature conductance, we take the derivative of the current equation with respect to voltage,  $G = \frac{2e}{h} \int dE T(E) \left(-\frac{\partial f}{\partial E}\right)$ , where  $f$  is the

Fermi-Dirac factor and  $T$  is the transmission probability. The relaxation and transmission calculations are both performed using a double numeric orbital basis to avoid any discrepancies that may arise using a single numeric basis [9]. Additional details on our approach can be found in Ref. [21].

We model the experimental CNT-molecule-CNT system in Ref. [1] using metallic (7,7) CNT contacts attached to the  $\pi$ -cruciform molecule [33] shown in Fig. 1. The molecule is referred to as molecule **1** in Ref. [1]. To build the structure, we begin by relaxing the isolated molecule with amide groups attached. We build the CNT out of optimized unit cells. We then cut the CNT to provide the closest fit to the molecule with amide linkers attached. We assume that after the etching step, the CNT contacts are fixed in their position and the molecular window is governed by the one-dimensional atomic layer spacing of the CNTs [1, 14]. We find that 9 unit cells of a (7,7) CNT are comparable in length to the relaxed molecule plus amide groups. At the dodecyloxybenzene cross-arm ring ends we attach a truncated  $C_2H_5$  alkane chain instead of  $C_{12}H_{25}$  used in the experiment since, being insulating, they do not affect the electronic properties of the conjugated central molecule. The system is constructed such that each CNT contact is at least 5 unit-cells in length on either side of the molecule. The CNT at the interface is passivated with hydrogen atoms to minimize localized surface states. We find that four CNT unit cells (8 atomic layers) for each CNT contact are long enough to damp out charge oscillations at the end layer (where the self-energies are added) that result from the C-H charge dipoles at the cut interfaces [21].

We show in Fig. 1 (B) a planar conformation of molecule **1** and in (C) a perpendicular conformation rotating only the cross-arm dodecyloxybenzene rings in each configuration. Both systems remain stable when relaxed with the plane of the amide groups at no more than 14.1 degrees from parallel to the tangential plane of the CNTs at the point of contact. This dihedral angle was found to have minimal effect on transmission up to 15 degrees from parallel [16]. The orientation of the planar molecule in Fig. 1 contrasts findings by Ke *et al.* modeling a comparable CNT-benzenediamide-CNT system [17]. Ke *et al.* found a low  $\pi$  orbital overlap between the (5,5) CNT contacts and molecule where the molecular plane was above the surface of two (5,5) CNTs. We find that the larger 1 nm diameter (7,7) CNT allows the amide linker to align nearly co-planarly with the CNT surface possibly due to a larger spacing between H atoms around CNT ends. The discrepancy could also be affected

by the different lengths of the molecules studied.

In Fig. 1 (A), we show the calculated transmission as a function of the difference  $E - E_F$  for the two structures. The transmission of the planar molecule has a resonant peak near the Fermi energy which results in a room temperature (300 K) resistance of 6.4 M $\Omega$ . The resistance of the perpendicular molecule is 1.6 G $\Omega$ . The experimental measured resistance is 5 M $\Omega$  [1].

To understand the difference in the transmission curves of the two molecules in Fig. 1, we examine the relaxed isolated molecular orbitals, shown in Fig. 2. Both molecules remain stable during relaxation with the planar conformation energetically favorable by 1.4 eV. Fig. 2 shows the LUMO, HOMO, HOMO-1, HOMO-2 and HOMO-3 (top to bottom) for both molecules with the amide groups attached at the left and right ends. The difference between the two molecules is notably the HOMO. In the planar conformation, the HOMO lies across the molecule perpendicular to the LUMO and the path of transport. The HOMO in the perpendicular conformation is localized strongly around the amide linkers and is oriented parallel to the LUMO. Because the  $\pi$ -conjugations extends across both arms of the cross in the planar molecule, the orbitals are more extended than in the perpendicular conformation. This spreading of the orbital wavefunction reduces the HOMO-LUMO gap to 1.69 eV in the planar conformation from 2.17 eV in the perpendicular conformation. The HOMO-1 and HOMO-2 states in both molecules are split by a few meV and are essentially degenerate.

We next compare the covariant spectral functions [21] at each transmission peak shown in Fig. 3 to the orbitals of the isolated molecules. The spectral function labels (1-4) correspond to the labeled transmission peaks in Fig. 1. The broad transmission peak (1) corresponds to the molecular LUMO in both systems. The broad transmission peak and the LUMO that extends across the entire CNT-molecule-CNT structure indicate that the coupling of the CNT orbital to the molecular LUMO is strong. This is consistent with results found by others [16, 17]. Peak (2) in the transmission curve results from the coupling of the CNT states to the HOMO of the planar molecule. This state is localized on the cross-arm of the molecule away from the CNTs and is weakly coupled to the contacts. The Fano resonance at peak (2) results from the two parallel paths through the molecule. An electron can tunnel through the tail of the extended state (1) or it can tunnel through the localized state (2). Transmission peak (3) results from the resonant tunneling through the degenerate HOMO-1 / HOMO-2 states of the planar molecule localized on the oxygen atoms linking

the dodecyloxybenzene rings to the  $C_2H_5$  alkane chains. Transmission peak (4) results from coupling to the HOMO-3 orbital of the planar molecule and the HOMO orbital of the perpendicular molecule. The spectral functions for peaks (1) and (4) are qualitatively the same for both molecular conformations, so we only show the spectral function of the planar molecule. Transmission peak (3) is also a Fano resonance arising from the two parallel paths corresponding to the HOMO-1 / HOMO-2 states localized on the cross-arms and the HOMO-3 state extended across the molecule. This comparison clearly maps the features in the transmission directly to the features of the isolated molecular orbitals.

The examinations of the transmission, molecular orbitals and spectral functions explains the difference in resistance of the two molecular conformations in Fig. 1. Rotating the the dodecyloxybenzene rings breaks the conjugation with the rings on the horizontal axis of the molecule and removes the HOMO localized on the cross-arms. The HOMO-LUMO gap widens leaving no states near the Fermi energy to carry current, and the resistance increases by over 2 orders of magnitude.

The use of conformation change for molecular switching is well known. Several examples are rotaxane [34, 35], 1,4-bis-phenylethynyl-benzene [10], and 2'-amino-4-ethylphenyl-4'-ethylphenyl-5'-nitro-1-benzenethiolate [36, 37] which we refer to as the nitro molecule. In all cases the conformation change of the molecules alters the molecular orbitals along the path of the electron transport. In the nitro molecule, the conjugation is broken directly in the transport path between each contact. In rotaxane, the orbital changes from extended to localized along the transmission path of the molecule. For the cruciform molecule, shown in Fig. 1, the effect of conformation is different. The rotation of the vertical rings does not affect the conjugation along the horizontal axis of the molecule, and it does not localize a previously extended state along the axis of the molecule. Instead, it removes the HOMO that lies on the cross rings, puts it back onto the horizontal axis of the molecule but at a lower energy resulting in exponentially decreased transmission near the Fermi energy and a several order of magnitude reduction in the conductance. This is a new twist on the conformation-change paradigm of molecular switching.

Experimentally it has been suggested that up to two molecular bridges might be established across the gap [1] during the dehydration reaction. While the molecular end groups on the cut ends of the CNTs are not known, it is reasonable to assume that the CNT ends remain functionalized with carboxyl groups (COOH), rather than H atoms, after de-

hydration reaction [1]. To explore these issues, we first add one additional molecule to our CNT-molecule-CNT system. Fig. 4 (A) shows a relaxed CNT-molecule-CNT system where an additional planar molecule is attached parallel to the original molecule shown in Fig. 1 (B). The maximally separated configuration of the two molecules shown here is known to be energetically favorable. [19]. The two molecule transmission is shown in Fig. 4 (B) where we observe a doubling of peaks near the Fermi level giving a calculated resistance of  $4.7\text{M}\Omega$ . As expected, the peaks are associated with the same orbitals previously discussed in relation to Figs. 1-3. The addition of one molecular bridge reduces the resistance, but not by a factor of two. The resistance is sensitive to the position of the HOMO resonant transmission peaks with respect to the Fermi level, and the two peaks from the two molecules split and shift compared to the single peak from a single molecule.

Finally, we cut a CNT non-vertically and passivate the side walls with carboxyl groups. We attach a single planar molecule shown in Fig. 4 (C) at the shortest portion of the molecular gap. The relaxed plane of the amide CONH groups is at no more than 24.2 degrees from parallel to the tangential plane of the CNTs at the point of contact. The transmission is shown in Fig. 4 (D) where the features remain qualitatively comparable to the features of the planar transmission in Fig. 1 (A). Quantitatively, we find a narrowing of each resonant peak. The LUMO and HOMO-3 peaks shift slightly deeper into the conductance and valence bands respectively. The spectral function at each peak again matches the features of the isolated molecular orbitals shown in Fig. 2. The calculated resistance is  $40\text{M}\Omega$ . The increase is the result of the narrowing of the HOMO resonance.

The transmission curve for the carboxyl passivated system contrasts to work done by Ren *et. al.* [19] where passivated carboxyl groups were compared to H passivation on semi-conducting (13,0) CNTs connected by a single diaminobenzene molecule. Ren *et. al.* found that the resonant peaks broaden in the valence and conduction band regions when the side-walls are passivated with carboxyl. The narrowing of the valence band resonances in our case, shown in Fig. 4 (D), indicate a lower coupling of the molecular states to the continuum of states in the CNT contacts. The decrease in coupling is partially due to the increased dihedral angle between the molecule and the plane of the CNT at the point of contact. The increase of the dihedral angle is caused by the increase of the steric hindrance of the carboxyl groups compared to the H atoms. The CNT sidewall chemistry, when relaxed, affects the orientation of the molecular junction due to negatively charged oxygen atoms on

the cut surface of the CNTs repelling the CONH linker oxygen atoms. This repulsion forces the amide horizontal axis to twist, affecting the  $\pi$ -bond overlap between the CNT contacts and the amide linkers.

We note that although the resistance has increased compared to the hydrogen passivation configuration, the overall transmission curve remains similar to the original system with the HOMO level near the Fermi energy. Overall the resistances listed in Table I are close to the experimental measurements, (excluding the perpendicular conformation). The proximity of the HOMO state near the Fermi energy provides a weakly-coupled transport path through the molecule at low bias regardless of the interface orientation, the number of molecular bridges, or the presence of carboxyl groups.

In summary, we have found good theoretical agreement with the first experimental measurement of a CNT-molecule-CNT system. The features in the transmission correspond directly to the features of the isolated molecular orbitals. The rotation of the dodecyloxy-benzene rings of the cross-arm alters the resistance by over 2 orders of magnitude even though it does not affect the conjugation along the transport path. The HOMO lying on the cross-arms of the planar molecule provides conductance at low bias that is relatively insensitive to the end groups of the cut CNTs, the cut angle, or the number of molecular bridges.

### **Acknowledgements**

This work is supported by the NSF (ECS-0524501) and the Semiconductor Research Corporation Focus Center Research Program on Nano Materials (FENA).

TABLE I: Resistance of four CNT-molecule-CNT systems studied where ‘Planar’ indicates the planar conformation of the molecule.

System	Conductance ( $M\Omega$ )
Perpendicular	1590
Planar	6.4
Planar / 2 molecules	4.7
Planar / carboxyl	40.
Experimental	5



## Figure Captions

Fig. 1. (A) Calculated transmission of the CNT-molecule-CNT structures where the solid line (red) is for the planar dodecyloxybenzene cross-arm conformation and the dashed line (blue) is for the perpendicular dodecyloxybenzene cross-arm conformation. (B and C) Relaxed CNT-molecule-CNT planar and perpendicular structures respectively.

Fig. 2. Calculated molecular orbitals for the isolated molecule in both the planar (left) and perpendicular (right) conformations. Amide groups are included at the left and right ends of each molecule.

Fig. 3. 3D contour plots of the covariant spectral function corresponding to the resonant transmission peaks marked in 1 calculated using the planar CNT-molecule-CNT structure.

Fig. 4. (A) CNT-molecule-CNT structure with two planar molecules attached. (B) Calculated transmission of CNT-molecule-CNT system shown in (A). (C) CNT-molecule-CNT structure with the CNT side walls passivated with carboxyl group molecules. (D) Calculated transmission of CNT-molecule-CNT system shown in (C).

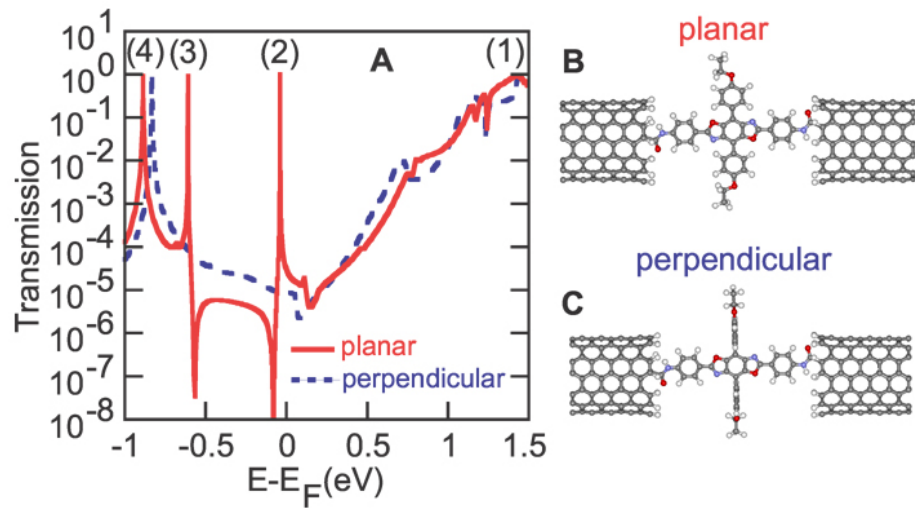


FIG. 1:

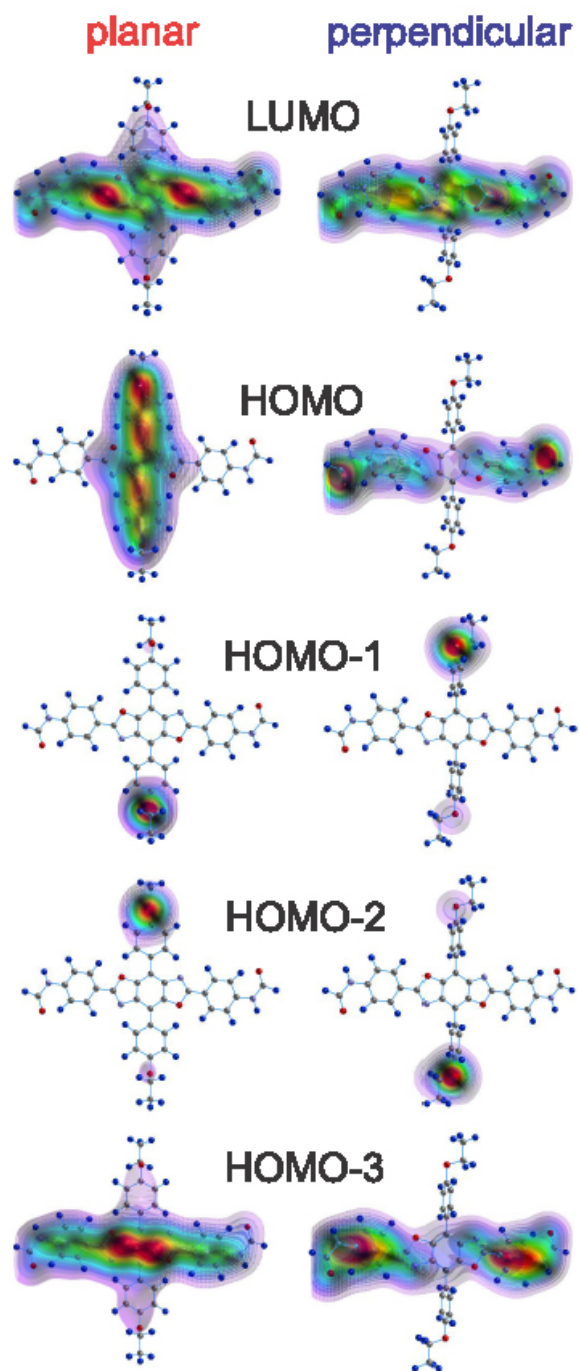


FIG. 2:

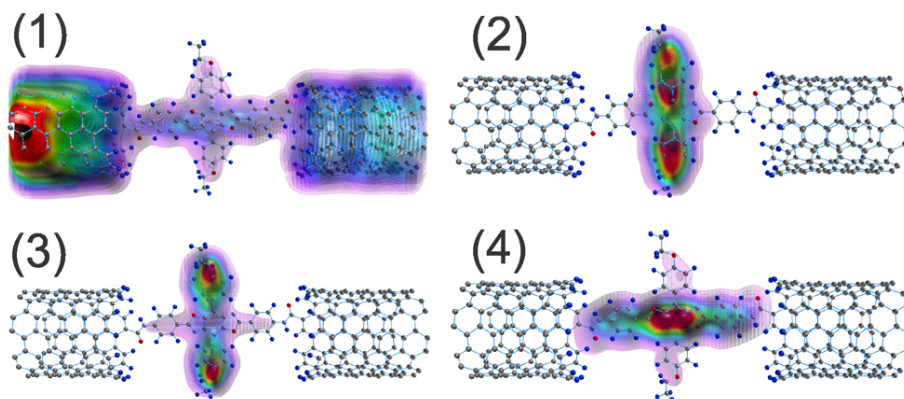


FIG. 3:

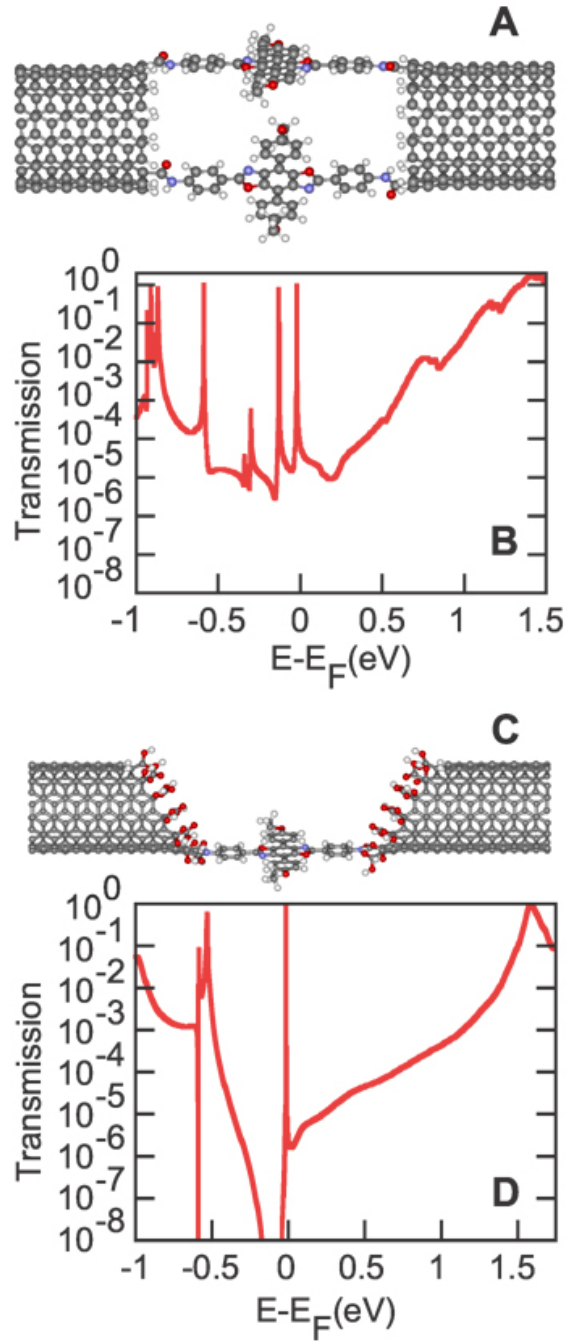


FIG. 4:

- 
- [1] X. Guo, J. P. Small, J. E. Klare, Y. Wang, M. S. Purewal, I. W. Tam, B. H. Hong, R. Caldwell, L. Huang, S. O'Brien, et al., *Science* **311**, 356 (2006), URL <http://www.sciencemag.org/cgi/content/abstract/311/5759/356>.
- [2] M. A. Reed, C. Zhou, C. J. Muller, T. P. Burgin, and J. M. Tour, *Science* **278**, 252 (1997).
- [3] J. Taylor, M. Brandbyge, and K. Stokbro, *Phys. Rev. Lett.* **89**, 138301/1 (2002).
- [4] P. Damle, A. Ghosh, and S. Datta, *Chem. Phys.* **281**, 171 (2002).
- [5] H. Basch, R. Cohen, and M. A. Ratner, *Nano Letters* **5**, 1668 (2005), URL <http://dx.doi.org/10.1021/nl1050702s>.
- [6] S. M. Lindsay and M. A. Ratner, *Adv. Mater.* **19**, 23 (2007).
- [7] C. C. Kaun and T. Seideman, *Phys. Rev. B* **77**, 033414 (2008).
- [8] S. Y. Quek, L. Venkataraman, H. J. Choi, S. G. Louie, M. S. Hybertsen, and J. B. Neaton, *Nano Lett.* **7**, 3477 (2007).
- [9] M. Strange, I. S. Kristensen, K. S. Thygesen, and K. W. Jacobsen, *J. Chem. Phys.* **128**, 114714 (2008).
- [10] J. Tomfohr and O. F. Sankey, *J. Chem. Phys.* **120**, 1542 (2004).
- [11] L. Venkataraman, J. E. Klare, C. Nuckolls, M. S. Hybertsen, and M. L. Steigerwald, *Nature* **442**, 904 (2006), URL [dx.doi.org/10.1038/nature05037](http://dx.doi.org/10.1038/nature05037).
- [12] L. Venkataraman, J. E. Klare, I. W. Tam, C. Nuckolls, M. S. Hybertsen, and M. L. Steigerwald, *Nano Lett.* **6**, 458 (2006), URL [dx.doi.org/10.1021/nl1052373+](http://dx.doi.org/10.1021/nl1052373+).
- [13] Z. Li and D. S. Kosov, *Phys. Rev. B* **76**, 035415 (2007), URL [dx.doi.org/10.1103/PhysRevB.76.035415](http://dx.doi.org/10.1103/PhysRevB.76.035415).
- [14] X. Guo, A. Whalley, J. E. Klare, L. Huang, S. O'Brien, M. Steigerwald, and C. Nuckolls, *Nano Letters* **7**, 1119 (2007).
- [15] J. He, B. Chen, A. K. Flatt, J. J. Stephenson, C. D. Doyle, and J. M. Tour, *Nature Mater.* **5**, 63 (2006).
- [16] Z. Qian, S. Hou, J. Ning, R. Li, Z. Shen, X. Zhao, and Z. Xu, *J. Chem. Phys.* **126**, 084705 (2007), URL [dx.doi.org/10.1063/1.2483760](http://dx.doi.org/10.1063/1.2483760).
- [17] S. H. Ke, H. U. Baranger, and W. Yang, *Phys. Rev. Lett.* **99**, 146802 (2007).
- [18] M. Valle, R. Gutierrez, C. Tejedor, and G. Cuniberti, *Nature Nanotech.* **2**, 176 (2007).

- [19] W. Ren, J. R. Reimers, N. S. Hush, Y. Zhu, J. Wang, and H. Guo, *J. Phys. Chem. C* **111**, 3700 (2007).
- [20] R. R. Pandey, N. Bruque, K. Alam, and R. Lake, *Phys. Stat. Sol. (a)* **203**, R5 (2006), URL <http://dx.doi.org/10.1002/pssa.200521467>.
- [21] N. A. Bruque, R. R. Pandey, and R. K. Lake, *Phys. Rev. B* **76**, 205322 (2007), URL <http://dx.doi.org/10.1103/PhysRevB.76.205322>.
- [22] B. Akdim and R. Pachter, *J. Phys. Chem. C* **112**, 3170 (2008).
- [23] H. Qian and J. Lu, *Physics Letters A* **371**, 465 (2007).
- [24] O. F. Sankey and D. J. Niklewski, *Phys. Rev. B* **40**, 3979 (1989).
- [25] J. P. Lewis, K. R. Glaesemann, G. A. Voth, J. Fritsch, A. A. Demkov, J. Ortega, and O. F. Sankey, *Phys. Rev. B* **64**, 195103 (2001).
- [26] P. Jelinek, H. Wang, J. P. Lewis, O. F. Sankey, and J. Ortega, *Phys. Rev. B* **71**, 235101 (2005).
- [27] P. A. Derosa and J. M. Seminario, *J. Phys. Chem. B* **105**, 471 (2001).
- [28] Y. Xue, S. Datta, and M. A. Ratner, *J. Chem. Phys.* **115**, 4292 (2001).
- [29] P. Damle, A. W. Ghosh, and S. Datta, *Phys. Rev. B* **64**, 201403(R) (2001).
- [30] Y. Xue, S. Datta, and M. A. Ratner, *Chem. Phys.* **281**, 151 (2002).
- [31] A. A. Demkov, J. Ortega, O. F. Sankey, and M. P. Grumbach, *Phys. Rev. B* **52**, 1618 (1995).
- [32] O. F. Sankey, A. A. Demkov, W. Windl, J. H. Fritsch, J. P. Lewis, and M. Fuentes-Cabrera, *Int. J. Quantum Chem.* **69**, 327 (1998).
- [33] J. E. Klare, G. S. Tulevski, and C. Nuckolls, *Langmuir* **20**, 10068 (2004).
- [34] A. H. Flood, J. F. Stoddart, D. W. Steuerman, and J. R. Heath, *Science* **306**, 2055 (2004).
- [35] S. S. Jang, Y. H. Jang, Y.-H. Kim, W. A. G. III, A. H. Flood, B. W. Laursen, H.-R. Tseng, J. F. Stoddart, J. O. Jeppesen, J. W. Choi, et al., *J. Am. Chem. Soc.* **127**, 1563 (2005).
- [36] M. A. Reed, J. Chen, A. M. Rawlett, D. W. Price, and J. M. Tour, *Appl. Phys. Lett.* **78**, 3735 (2001).
- [37] J. Chen and M. A. Reed, *Chem. Phys.* **281**, 127 (2002).